Advances in Nano Research, *Vol. 7 No. 5 (2019) 325-335*
DOI: https://doi.org/10.12989/anr.2019.7.5.325

Dispersion of waves in FG porous nanoscale plates based on NSGT in thermal environment

Farzad Ebrahimi [*1], Ali Seyfi [1] and Ali Dabbagh [2]

[1] *Department of Mechanical Engineering, Faculty of Engineering, Imam Khomeini International University, Qazvin, Iran*
[2] *School of Mechanical Engineering, College of Engineering, University of Tehran, Tehran, Iran*

(*Received March 21, 2019, Revised July 19, 2019, Accepted August 10, 2019*)

Abstract. In the present study, nonlocal strain gradient theory (NSGT) is developed for wave propagation of functionally graded (FG) nanoscale plate in the thermal environment by considering the porosity effect. Si_3N_4 as ceramic phase and SUS304 as metal phase are regarded to be constitutive material of FG nanoplate. The porosity effect is taken into account on the basis of the newly extended method which considers coupling influence between Young's modulus and mass density. The motion relation is derived by applying Hamilton's principle. NSGT is implemented in order to account for small size effect. Wave frequency and phase velocity are obtained by solving the problem via an analytical method. The effects of different parameters such as porosity coefficient, gradient index, wave number, scale factor and temperature change on phase velocity and wave frequency of FG porous nanoplate have been examined and been presented in a group of illustrations.

Keywords: wave propagation; nonlocal strain gradient theory; thermal environment; porosity-dependent homogenization

1. Introduction

From past to present, scientists and researchers always wanted to find material with wonderful properties to using in industrial sciences. Thus, they have studied the properties of different materials for years to choose the best material as it is possible. Functionally Graded Material (FGM) is one of the novel materials which researchers discovered it. In the mid-1980s Japanese's scientists have figured it out and they realized that this material has supreme features such as high temperature resistance, high strength and improved corrosion resistance. This kind of materials is a novel generation which is microscopically nonhomogeneous will be attained by administering the volume fractions, microstructure, porosity, and other parameters of the material constituents during the manufacturing procedure. Fabrication of such materials leads to spatial gradient of macroscopic material properties such as thermal conductivity and mechanical strength.

Normally, FGM includes two phases, metal phase that resists fracture that is caused by thermal stresses and ceramic phase that can tolerate the intense thermal loading. Also, owing to the existence of two phases, mechanical properties vary through the thickness direction. Besides, FGMs have many advantages that attracted the researchers' attention. These materials are utilized in various engineering fields like aerospace structures, military aircraft propulsion system and others. The mentioned points are sufficient to persuade scientists to investigate on characteristics of FGM structures and analyses of their behavior (Aydogdu and Taskin 2007, Azadi 2011, Şimşek and Reddy 2013, Hebali *et al.* 2014, Li *et al.* 2015, Hosseini and Rahmani 2016, Ebrahimi and Haghi 2017). For example, Thanh *et al.* (2017) investigated the effect of thermal loading on nonlinear dynamic and vibration behavior of imperfect functionally graded carbon nanotube reinforced composite (FG-CNTRC) plates resting on elastic foundations under dynamic in the framework of third-order shear deformation plate theory. The nonlinear vibration responses of FG-CNTRC annular plates with integrated piezoelectric layers resting on Pasternak foundation is discussed by Keleshteri *et al.* (2017). Ebrahimi *et al.* (2017b) have probed vibration analysis of magneto-electro-elastic (MEE) heterogeneous porous material plates resting on elastic medium. Also, thermal loading effect on wave propagation analysis of a temperature-dependent FG rotating nanosize beam under based on NSGT is carried out by Ebrahimi *et al.* (2017a). Free vibration characteristics of FGM sandwich doubly-curved shallow shells has been presented by Chen *et al.* (2017) under simply supported conditions. On the basis of the refined four-variable plate theory, Ebrahimi *et al.* (2018a) explored wave propagation behavior of an embedded FG nanoplate by considering the thermal loading effect. Thermal environments effect on the nonlinear forced vibrational analysis of FG laminated composite plates reinforced with graphene layers rested on the viscoelastic foundation is surveyed by Fan *et al.* (2018). Eringen's nonlocal elasticity theory is employed by Ebrahimi *et al.* (2018b) to investigate wave propagation response of a rotating FGM nanobeam. Shahsavari *et al.* (2018) studied free vibration analysis of FG porous plates resting on elastic foundations using quasi-3D hyperbolic theory. Lv *et al.* (2018) have studied the effect of the

*Corresponding author, Associate Professor,
E-mail: febrahimy@eng.ikiu.ac.ir

ISSN: 2287-237X (Print), 2287-2388 (Online)

material defects on the nonlinear vibrational response of embedded FG nanobeams based on NSGT. Bending, buckling and free vibration characteristics of incompressible FG plates have been carried out by Mohammadi *et al.* (2019) employing both higher order shear and normal deformable plate theory. Zeng *et al.* (2019) have analyzed the influence of electrical load on nonlinear vibration analysis of piezoelectric sandwich nanoplates made of FG porous core.

Porosity is a measure of the void and one of the destructive factors which can affect the mechanical properties of materials including FGMs. Porosity is usually made through the manufacturing process. It is worth mentioning that analyzing porosity effect can be surely beneficial in investigating the materials' mechanical behavior. Accordingly, many scientists have studied the effect of porosity in their investigations. For example, the vibrational behavior of FG beams made of porous material under different thermal loadings is carried out by Ebrahimi *et al.* (2016b). Moreover, Eltaher *et al.* (2018) examined bending and vibration responses of FG porous nanobeams implementing a modified porosity model using the finite element method. This porosity model represents the relation between density and the elastic modulus and porosity parameter. Phung-Van *et al.* (2019) discussed nonlinear transient analysis of FG porous nanoscale plates within the framework of higher order shear deformation theory. Free and forced vibration analysis of a porous nanoshell reinforced by graphene platelets is investigated by Pourjabari *et al.* (2019).

In the last decade, nanotechnology and nano materials have attracted the attention of many scientists. Hence, they performed a lot of researches on the behavior of nanostructures and they have found out that behavior of nanoscale structures possesses size dependency and also owing to the inefficiency of the classical continuum theory in precisely forecasting the dynamic response mechanical properties, it cannot be used for nano structures. As a result, there are various continuum theories which have been developed and applied to capture correctly size-dependent behavior of nano structures. These theories can help scientists to take into account the size effects in mechanical analysis of nanoscale material and structures. NSGT and nonlocal elasticity are two theories that many researchers use them to explore size effects in their investigations. Li *et al.* (2015) have developed an analytic model of small-scaled FG beams for the flexural wave propagation analysis based on NSGT. Size-dependent free vibration analysis of nanoplates made of FGMs has been investigated by Daneshmehr *et al.* (2015) based on nonlocal elasticity theory with high order theories. Ebrahimi *et al.* (2016a) have studied the wave propagation of an inhomogeneous FG nanoplate subjected to nonlinear thermal loading by the means of NSGT. Electromechanical buckling of beam-type nanoelectromechanical systems (NEMSs) has been studied by Shojaeian *et al.* (2016) based on modified strain gradient theory. A novel size-dependent beam model has been proposed for nonlinear free vibration of FG nanobeam with immovable ends based on NSGT and Euler-Bernoulli beam theory in conjunction with the von-Kármán's geometric nonlinearity has been described by Şimşek (2016). NSGT has been used by Ebrahimi and Dabbagh (2017) to capture size effects in wave propagation analysis of compositionally graded smart nanoplates and Ebrahimi and Barati (2017) have investigated buckling characteristics of a curved FG nanobeam based on NSGT accounting the stress for not only the nonlocal stress field but also the strain gradients stress field. Zeighampour *et al.* (2018) have investigated wave propagation in viscoelastic single-walled carbon nanotubes by accounting for the simultaneous effects of the nonlocal constant and the material length scale parameter. Nonlocal strain gradient shell model has been used by Sahmani and Aghdam (2018) for axial buckling and postbuckling analysis of MEE composite nanoshells. A size-dependent nonlinear nonlocal strain gradient model for nanoscale tubes has been proposed by Ghayesh and Farajpour (2018) and the forced mechanical behavior has been examined by Barati (2018) modeling the Dynamic model of nanoplates constructed from porous FG and metal foam materials based on NSGT. Fuschi *et al.* (2019) have studied Size effects of small-scale beams in bending addressed with a strain-difference based nonlocal elasticity theory. Based on the NSGT and surface elasticity theory, a unified size-dependent plate model has been developed by Lu *et al.* (2019) for buckling analysis of rectangular nanoplates. Tan and Chen (2019) have described the size-dependent electro-thermo-mechanical analysis of multilayer cantilever microactuators by Joule heating have used the modified couple stress theory. Ebrahimi *et al.* (2019a) employed Eringen's nonlocal elasticity theory for wave propagation behavior of MEE nanotube considering shell model.

On the other hand, there are not many articles that wave propagation of porous nano structures based on the different theories have been investigated in them. A general bi-Helmholtz nonlocal strain-gradient elasticity model has been developed for wave dispersion analysis of porous double-nanobeam systems in thermal environments by Barati (2017) and Mahinzare *et al.* (2019) investigated vibrational behavior of functionally graded piezoelectric material in a nano circular plate subjected to rotational and thermal loads based on NSGT. Based on NSGT, Mirjavadi *et al.* (2019) have transient behavior of a porous FG nanoplate due to various impulse loads has been studied. Ebrahimi *et al.* (2019b) have just examined porosity influence on wave dispersion behavior of FG nanobeam according to NSGT.

As mentioned above, we have lots of researches in the field of wave propagation of FG nanostructures but nobody has investigated wave propagation analysis of FG porous nanoscale plate based on the NSGT in thermal environment.

In this paper, we have studied wave propagation analysis of FGM by using NSGT to consider the size effects in nano scales. To find the equations of motion of the FG porous nanoscale plate, we used Hamilton's principle. Temperature dependent is considered by solving a heat conduction problem through the thickness of the nanoscale plate and in our porosity model that we considered mass density and Young's modulus have a direct relationship together.

2. Theory and formulation

2.1 Modified power-law homogenization method

First, equivalent mechanical properties of FG nanoplate by considering porosity effect is covered on the basis of a modified porosity dependent homogenization scheme which shows porosity affects wave propagation responses of FG nanoplates significantly. By searching in literature, it can be found out that in all similar works that explored porosity effects on equivalent material properties, a linear function is considered for the porosity effect. Although this method can describe the decreasing impact of porosity, it cannot be assumed as a realistic homogenization method for the purpose of regarding porosity effects (Zok and Levi 2001). The present method relates the effective Young's modulus of porous FGMs to the mass densities of both perfect and porous materials. Moreover, the homogenization is constructed based on the primary definition of porosity. The equivalent material properties can be expressed in the following form

$$E(z) = (E_C - E_M)\left(\frac{z}{h} + \frac{1}{2}\right)^P + E_M - \left(\frac{m_0 - m_1}{m_0}\right)(E_C + E_M) \tag{1}$$

$$\rho(z) = (\rho_C - \rho_M)\left(\frac{z}{h} + \frac{1}{2}\right)^P + \rho_M - \frac{\alpha}{2}(\rho_C + \rho_M) \tag{2}$$

where E and ρ denote Young's modulus and mass density of FG nanoplate, respectively. In addition, C and M subscripts are ceramic and metal phases, respectively. The power exponent P is defined for the goal of tuning the volume fraction of ceramic and metallic phases of the implemented FGM. In fact, the higher is the power exponent, the greater will be the volume fraction of the ceramic-rich phase. Also, α is the porosity volume fraction. Also, m_0 and m_1 are the true and apparent mass densities, respectively and can be computed as

$$m_0 = \int_{-h/2}^{h/2} \rho(z)\, dz \qquad at \quad \alpha = 0 \tag{3a}$$

$$m_1 = \int_{-h/2}^{h/2} \rho(z)\, dz \qquad at \quad \alpha > 0 \tag{3b}$$

Temperature-dependent coefficients of material phases can be written as

$$X = X_0(1 + X_{-1} + X_2 + X_3) \tag{4}$$

In which X_0, X_{-1}, X_1, X_2 and X_3 stand for temperature-dependent coefficients that are presented in Table 1 for *Si_3N_4* and *SUS304*. The top and bottom surfaces of FG nanoplate are fully ceramic (*Si_3N_4*) and fully metal (*SUS304*), respectively. In this paper, it is presumed that the temperature varies nonlinearly through the thickness of plate. Temperature distribution can be achieved by solving the steady-state heat conduction equation with respect to boundary conditions on the top and bottom surfaces of nanoplate across the thickness

$$-\frac{d}{dz}\left(K(z,T)\frac{dT}{dz}\right) = 0 \tag{5}$$

Regarding

$$T\left(\frac{h}{2}\right) = T_C \tag{6a}$$

$$T\left(-\frac{h}{2}\right) = T_M \tag{6b}$$

By solving the noted equation, temperature function can be formulated as follow

$$T = T_M + (T_C - T_M)\frac{\int_{-\frac{h}{2}}^{z}\frac{1}{K(z,T)}dz}{\int_{-\frac{h}{2}}^{\frac{h}{2}}\frac{1}{K(z,T)}dz} \tag{7}$$

Table 1 Temperature-dependent coefficients for Si_3N_4 and SUS304 (Ebrahimi *et al.* 2016a)

Material	Properties	X_0	X_{-1}	X_1	X_2	X_3
Si_3N_4	E (Pa)	348.43e+9	0	−3.070e-4	2.160e-7	−8.946e-11
	α (K^{-1})	5.8723e-6	0	9.095e-4	0	0
	ρ (Kg/m^3)	2370	0	0	0	0
	κ (W/mK)	13.723	0	−1.032e-3	5.466e-7	−7.876e-11
	ν	0.24	0	0	0	0
SUS304	E (Pa)	201.04e + 9	0	3.079e-4	−6.534e-7	0
	α (K^{-1})	12.330e-6	0	8.086e-4	0	0
	ρ (Kg/m^3)	8166	0	0	0	0
	κ (W/mK)	15 .379	0	−1.264e-3	2.092e-6	−7.223e-10
	ν	0.3262	0	−2.002e-4	3.797e-7	0

2.2 Kinetic relations

According to refined shear deformation plate theories, the displacement field of nonlocal FGM nanoscale plate can be written as

$$u(x,y,z,t) = u_0(x,y,t) - z\frac{\partial w_b(x,y,t)}{\partial x} - f(z)\frac{\partial w_s(x,y,t)}{\partial x} \tag{8}$$

$$v(x,y,z,t) = v_0(x,y,t) - z\frac{\partial w_b(x,y,t)}{\partial x} - f(z)\frac{\partial w_s(x,y,t)}{\partial x} \tag{9}$$

$$w(x,y,z,t) = w_b(x,y,t) + w_s(x,y,t)` \tag{10}$$

where u_0 and v_0 are longitudinal and transverse displacements and w_b and w_s indicate bending deflection and shear deflection, respectively. Plus, $f(z)$ is the shape function which demonstrates distribution of shear stress and strain through the thickness direction. The shape function can be presented as

$$f(z) = z - \frac{\sin(\zeta z)}{\zeta} \tag{11}$$

in which $\zeta = \frac{z}{h}$. Furthermore, the nonzero strains of the using theory can be calculated in the following form

$$\begin{Bmatrix}\varepsilon_x\\ \varepsilon_y\\ \gamma_{xy}\end{Bmatrix} = \begin{Bmatrix}\varepsilon_x^0\\ \varepsilon_y^0\\ \gamma_{xy}^0\end{Bmatrix} + z\begin{Bmatrix}k_x^b\\ k_y^b\\ k_{xy}^b\end{Bmatrix} + f(z)\begin{Bmatrix}k_x^s\\ k_y^s\\ k_{xy}^s\end{Bmatrix}, \quad \begin{Bmatrix}\gamma_{xz}\\ \gamma_{yz}\end{Bmatrix} = \begin{Bmatrix}\gamma_{xz}^0\\ \gamma_{yz}^0\end{Bmatrix} \tag{12}$$

Where

$$\begin{Bmatrix}\varepsilon_x^0\\ \varepsilon_y^0\\ \gamma_{xy}^0\end{Bmatrix} = \begin{Bmatrix}\frac{\partial u_0}{\partial x}\\ \frac{\partial v_0}{\partial x}\\ \frac{\partial u_0}{\partial x} + \frac{\partial v_0}{\partial x}\end{Bmatrix}, \quad \begin{Bmatrix}k_x^b\\ k_y^b\\ k_{xy}^b\end{Bmatrix} = \begin{Bmatrix}-\frac{\partial^2 w_b}{\partial x^2}\\ -\frac{\partial^2 w_b}{\partial y^2}\\ -2\frac{\partial w_b}{\partial x \partial y}\end{Bmatrix}$$
$$\begin{Bmatrix}k_x^s\\ k_y^s\\ k_{xy}^s\end{Bmatrix} = \begin{Bmatrix}-\frac{\partial^2 w_s}{\partial x^2}\\ -\frac{\partial^2 w_s}{\partial y^2}\\ -2\frac{\partial w_s}{\partial x \partial y}\end{Bmatrix}, \quad \begin{Bmatrix}\gamma_{xz}^0\\ \gamma_{yz}^0\end{Bmatrix} = \begin{Bmatrix}\frac{\partial w_s}{\partial x}\\ \frac{\partial w_s}{\partial y}\end{Bmatrix} \tag{13}$$

Next, in order to achieve the Euler–Lagrange equations of FG porous nanoplate, Hamilton's principle has been employed that is presented as follow

$$\int_{t_0}^{t_1} \delta(U - T + V)dt = 0 \tag{14}$$

where δU, δT and δV denote variation of strain energy, kinetic energy work done by external loadings, respectively. Now, the variation of strain energy can be written as

$$\delta U = \int_V \begin{pmatrix}\sigma_x\delta\varepsilon_x + \sigma_y\delta\varepsilon_y + \tau_{xy}\delta\gamma_{xy}\\ +\tau_{xz}\delta\gamma_{xz} + \tau_{yz}\delta\gamma_{yz}\end{pmatrix} dV \tag{15}$$

By substituting Eqs. (12), (13) in Eq. (15), the strain energy can be calculated as

$$\delta U = \int_0^L \begin{pmatrix}N_x\delta\varepsilon_x^0 + N_y\delta\varepsilon_y^0 - M_x^b\kappa_x^b - M_x^s\kappa_x^s\\ -M_y^b\kappa_y^b - M_y^b\kappa_y^s + N_{xy}\delta\gamma_{xy}^0\\ +M_{xy}^b k_{xy}^b + M_{xy}^s k_{xy}^s\\ +Q_{yz}\frac{\partial\delta w_s}{\partial y} + Q_{xz}\frac{\partial\delta w_s}{\partial x}\end{pmatrix} dx \tag{16}$$

in which the stress resultants N, M and Q are defined by

$$\left[N_j, M_j^b, M_j^s\right] = \int_A [1, z, f(z)]\,\sigma_j dA, \quad j = (x,y,xy) \tag{17}$$

$$Q_j = \int_A g(z)\,\sigma_j dA, \qquad j = (x,y,xy) \tag{18}$$

where, $g(z) = 1 - \frac{df(z)}{dz}$.

the variation of kinetic energy can be expressed as

$$\delta T = \int (\ddot{u}\delta u + \ddot{v}\delta v + \ddot{w}\delta w)\rho(z)dV = \int_0^L \begin{bmatrix} I_0(\ddot{u}\delta u + \ddot{v}\delta v + (\ddot{w}_b + \ddot{w}_s)\delta(w_b + w_s)\\ -I_1\left(\ddot{u}\frac{\partial\delta w_b}{\partial x} + \delta\ddot{u}\frac{\partial w_b}{\partial x} + \ddot{v}\frac{\partial\delta w_b}{\partial y} + \delta\ddot{v}\frac{\partial w_b}{\partial y}\right)\\ -J_1\left(\ddot{u}\frac{\partial\delta w_s}{\partial x} + \delta\ddot{u}\frac{\partial w_s}{\partial x} + \ddot{v}\frac{\partial\delta w_s}{\partial y} + \delta\ddot{v}\frac{\partial w_s}{\partial y}\right)\\ +I_2\left(\frac{\partial\delta w_b}{\partial x}\frac{\partial w_b}{\partial x} + \frac{\partial\delta w_b}{\partial y}\frac{\partial w_b}{\partial y}\right)\\ +K_2\left(\frac{\partial w_s}{\partial x}\frac{\partial\delta w_s}{\partial x} + \frac{\partial w_s}{\partial y}\frac{\partial\delta w_s}{\partial y}\right)\\ +J_2\left(\begin{array}{l}\frac{\partial\ddot{w}_b}{\partial x}\frac{\partial\delta w_s}{\partial x} + \frac{\partial\delta\ddot{w}_b}{\partial x}\frac{\partial w_s}{\partial x}\\ +\frac{\partial\ddot{w}_b}{\partial y}\frac{\partial\delta w_s}{\partial y} + \frac{\partial\delta\ddot{w}_b}{\partial y}\frac{\partial w_s}{\partial y}\end{array}\right) \end{bmatrix} dx \tag{18}$$

where the mass moment of inertias can be computed via

$$[I_0, I_1, I_2, J_1, J_2, K_2] = \int_A [1, z, z^2, f(z), zf(z), f^2(z)]\rho(z)dA \tag{19}$$

The variation of work done by applied forces can be expressed in the following form

$$\delta V = \int_0^L N^T \left(\begin{matrix} \frac{\partial (w_b + w_s)}{\partial x} \frac{\partial \delta (w_b + w_s)}{\partial x} \\ + \frac{\partial (w_b + w_s)}{\partial y} \frac{\partial \delta (w_b + w_s)}{\partial y} \end{matrix} \right) dx \quad (20)$$

Where

$$N^T = \int_{-\frac{h}{2}}^{\frac{h}{2}} \frac{E(z)}{1-\nu} \alpha(z,T)(T - T_0) dz \quad (21)$$

By inserting Eqs. (16), (18) and (20) into Eq. (14) and setting the coefficients of $\delta u_0,\ \delta v_0, \delta w_b, \delta w_s$ to zero, the Euler-Lagrange equations of a FG sinusoidal plate are attained as

$$\frac{\partial N_x}{\partial x} + \frac{\partial N_{xy}}{\partial x} = I_0 \ddot{u}_0 - I_1 \frac{\partial \ddot{w}_b}{\partial x} - J_1 \frac{\partial \ddot{w}_s}{\partial x} \quad (22)$$

$$\frac{\partial N_y}{\partial y} + \frac{\partial N_{xy}}{\partial x} = I_0 \ddot{v}_0 - I_1 \frac{\partial \ddot{w}_b}{\partial y} - J_1 \frac{\partial \ddot{w}_s}{\partial y} \quad (23)$$

$$\begin{aligned} &\frac{\partial^2 M_x^b}{\partial x^2} + 2\frac{\partial^2 M_{xy}^b}{\partial x \partial y} + \frac{\partial^2 M_y^b}{\partial y^2} - N^T \nabla^2 (w_b + w_s) \\ &= I_0 (\ddot{w}_b + \ddot{w}_s) + I_1 \left(\frac{\partial \ddot{u}}{\partial x} + \frac{\partial \ddot{v}}{\partial y} \right) - I_2 \nabla^2 \ddot{w}_b - J_2 \nabla^2 \ddot{w}_s \end{aligned} \quad (24)$$

$$\begin{aligned} &\frac{\partial^2 M_x^s}{\partial x^2} + 2\frac{\partial^2 M_{xy}^s}{\partial x \partial y} + \frac{\partial^2 M_y^s}{\partial y^2} + \frac{\partial Q_{xz}}{\partial x} \\ &+ \frac{\partial Q_{yz}}{\partial y} - N^T \nabla^2 (w_b + w_s) \\ &= I_0 (\ddot{w}_b + \ddot{w}_s) + J_1 \left(\frac{\partial \ddot{u}}{\partial x} + \frac{\partial \ddot{v}}{\partial y} \right) - J_2 \nabla^2 \ddot{w}_b - K_2 \nabla^2 \ddot{w}_s \end{aligned} \quad (25)$$

2.3 The nonlocal strain gradient theory

Based on size-dependent continuum theory the stress-strain relationship in FG nanoplates is found and it should be mixed stress-strain relation with Euler-Lagrange equations in order to gather the nonlocal governing equations of problem. Accordingly, NSGT is implemented for FG porous nanoplate and can be defined in the following form

$$(1 - \mu^2 \nabla^2)\sigma = (1 - \lambda^2 \nabla^2) C : \varepsilon \quad (26)$$

where μ, λ and C are nonlocal and length scale parameters and elasticity tensor, respectively. Also, in above equation, ∇^2 stands for Laplacian operator which can be described as

$$\nabla^2 = \frac{\partial^2}{\partial x^2} + \frac{\partial^2}{\partial y^2} \quad (27)$$

the stress-strain relationships of a refined plate can be modified as follow

$$\begin{aligned} &(1 - \mu^2 \nabla^2) \begin{Bmatrix} N_x \\ N_y \\ N_{xy} \end{Bmatrix} \\ &= (1 - \lambda^2 \nabla^2) \left[\begin{bmatrix} A_{11} & A_{12} & 0 \\ A_{21} & A_{22} & 0 \\ 0 & 0 & A_{33} \end{bmatrix} \begin{Bmatrix} \frac{\partial u_0}{\partial x} \\ \frac{\partial v_0}{\partial x} \\ \frac{\partial u_0}{\partial x} + \frac{\partial v_0}{\partial x} \end{Bmatrix} \right. \\ &+ \begin{bmatrix} B_{11} & B_{12} & 0 \\ B_{21} & B_{22} & 0 \\ 0 & 0 & B_{66} \end{bmatrix} \begin{Bmatrix} -\frac{\partial^2 w_b}{\partial x^2} \\ -\frac{\partial^2 w_b}{\partial y^2} \\ -2\frac{\partial w_b}{\partial x \partial y} \end{Bmatrix} \\ &\left. + \begin{bmatrix} B_{11}^s & B_{12}^s & 0 \\ B_{21}^s & B_{22}^s & 0 \\ 0 & 0 & B_{66}^s \end{bmatrix} \begin{Bmatrix} -\frac{\partial^2 w_s}{\partial x^2} \\ -\frac{\partial^2 w_s}{\partial y^2} \\ -2\frac{\partial w_s}{\partial x \partial y} \end{Bmatrix} \right] \end{aligned} \quad (28)$$

$$\begin{aligned} &(1 - \mu^2 \nabla^2) \begin{Bmatrix} M_x^b \\ M_y^b \\ M_{xy}^b \end{Bmatrix} \\ &= (1 - \lambda^2 \nabla^2) \left[\begin{bmatrix} B_{11} & B_{12} & 0 \\ B_{21} & B_{22} & 0 \\ 0 & 0 & B_{66} \end{bmatrix} \begin{Bmatrix} \frac{\partial u_0}{\partial x} \\ \frac{\partial v_0}{\partial x} \\ \frac{\partial u_0}{\partial x} + \frac{\partial v_0}{\partial x} \end{Bmatrix} \right. \\ &+ \begin{bmatrix} D_{11} & D_{12} & 0 \\ D_{21} & D_{22} & 0 \\ 0 & 0 & D_{66} \end{bmatrix} \begin{Bmatrix} -\frac{\partial^2 w_b}{\partial x^2} \\ -\frac{\partial^2 w_b}{\partial y^2} \\ -2\frac{\partial w_b}{\partial x \partial y} \end{Bmatrix} \\ &\left. + \begin{bmatrix} D_{11}^s & D_{12}^s & 0 \\ D_{21}^s & D_{22}^s & 0 \\ 0 & 0 & D_{66}^s \end{bmatrix} \begin{Bmatrix} -\frac{\partial^2 w_s}{\partial x^2} \\ -\frac{\partial^2 w_s}{\partial y^2} \\ -2\frac{\partial w_s}{\partial x \partial y} \end{Bmatrix} \right] \end{aligned} \quad (29)$$

$$(1-\mu^2\nabla^2)\begin{Bmatrix} M_x^s \\ M_y^s \\ M_{xy}^s \end{Bmatrix} = (1-\lambda^2\nabla^2)\left[\begin{bmatrix} B_{11}^s & B_{12}^s & 0 \\ B_{21}^s & B_{22}^s & 0 \\ 0 & 0 & B_{66}^s \end{bmatrix}\begin{Bmatrix} \dfrac{\partial u_0}{\partial x} \\ \dfrac{\partial v_0}{\partial x} \\ \dfrac{\partial u_0}{\partial x}+\dfrac{\partial v_0}{\partial x} \end{Bmatrix}\right.$$
$$+\begin{bmatrix} D_{11}^s & D_{12}^s & 0 \\ D_{21}^s & D_{22}^s & 0 \\ 0 & 0 & D_{66}^s \end{bmatrix}\begin{Bmatrix} -\dfrac{\partial^2 w_b}{\partial x^2} \\ -\dfrac{\partial^2 w_b}{\partial y^2} \\ -2\dfrac{\partial w_b}{\partial x \partial y} \end{Bmatrix} \tag{30}$$
$$\left.+\begin{bmatrix} H_{11}^s & H_{12}^s & 0 \\ H_{21}^s & H_{22}^s & 0 \\ 0 & 0 & H_{66}^s \end{bmatrix}\begin{Bmatrix} -\dfrac{\partial^2 w_s}{\partial x^2} \\ -\dfrac{\partial^2 w_s}{\partial y^2} \\ -2\dfrac{\partial w_s}{\partial x \partial y} \end{Bmatrix}\right]$$

$$(1-\mu^2\nabla^2)\begin{Bmatrix} Q_x \\ Q_y \end{Bmatrix} = (1-\lambda^2\nabla^2)\left[\begin{bmatrix} A_{44}^s & 0 \\ 0 & A_{55}^s \end{bmatrix}\begin{Bmatrix} \dfrac{\partial w_s}{\partial x} \\ \dfrac{\partial w_s}{\partial y} \end{Bmatrix}\right] \tag{31}$$

In the aforesaid equations the cross sectional rigidities are given as follow

$$\begin{Bmatrix} A_{11} & B_{11} & B_{11}^s & D_{11} & D_{11}^s & H_{11}^s \\ A_{12} & B_{12} & B_{12}^s & D_{12} & D_{12}^s & H_{12}^s \\ A_{66} & B_{66} & B_{66}^s & D_{66} & D_{66}^s & H_{66}^s \end{Bmatrix} = \int_A [1, z, z^2, f(z), zf(z), f^2(z)]\frac{E(z)}{1-\nu^2}\begin{Bmatrix} 1 \\ \nu \\ 1-\nu \end{Bmatrix} dA \tag{32a}$$

$$(A_{22}\ \ B_{22}\ \ B_{22}^s\ \ D_{22}\ \ D_{22}^s\ \ H_{22}^s) = (A_{11}\ \ B_{11}\ \ B_{11}^s\ \ D_{11}\ \ D_{11}^s\ \ H_{11}^s) \tag{32b}$$

$$A_{44}^s = A_{55}^s \int_A g^2(z)G(z)dA \tag{32c}$$

where $G(z) = \dfrac{E(z)}{2(1+\nu)}$.

By coupling above relations with Euler-Lagrange equations can be reached to the nonlocal governing equations of FG porous nanoplate. For this goal, Eqs. (26)-(29) are superseded in Eqs. (22)-(25) and the governing equations can be obtained as

$$(1-\lambda^2\nabla^2)\begin{pmatrix} A_{11}\dfrac{\partial^2 u_0}{\partial x^2}+A_{66}\dfrac{\partial^2 u_0}{\partial y^2}+(A_{12}+A_{66})\dfrac{\partial^2 v_0}{\partial x \partial y} \\ -B_{11}\dfrac{\partial^3 w_b}{\partial x^3}-(B_{12}+2B_{66})\dfrac{\partial^3 w_b}{\partial x \partial y^2} \\ -B_{11}^s\dfrac{\partial^3 w_s}{\partial x^3}-(B_{12}^s+2B_{66}^s)\dfrac{\partial^3 w_s}{\partial x \partial y^2} \end{pmatrix} + (1-\mu^2\nabla^2)\left(-I_0\ddot{u}_0+I_1\frac{\partial \ddot{w}_b}{\partial x}+J_1\frac{\partial \ddot{w}_s}{\partial x}\right)=0 \tag{33}$$

$$(1-\lambda^2\nabla^2)\begin{pmatrix} A_{22}\dfrac{\partial^2 v_0}{\partial y^2}+A_{66}\dfrac{\partial^2 v_0}{\partial x^2}+(A_{12}+A_{66})\dfrac{\partial^2 u_0}{\partial x \partial y} \\ -B_{22}\dfrac{\partial^3 w_b}{\partial y^3}-(B_{12}+2B_{66})\dfrac{\partial^3 w_b}{\partial x^2 \partial y} \\ -B_{22}^s\dfrac{\partial^3 w_s}{\partial y^3}-(B_{12}^s+2B_{66}^s)\dfrac{\partial^3 w_s}{\partial x^2 \partial y} \end{pmatrix} + (1-\mu^2\nabla^2)\left(-I_0\ddot{v}_0+I_1\frac{\partial \ddot{w}_b}{\partial y}+J_1\frac{\partial \ddot{w}_s}{\partial y}\right)=0 \tag{34}$$

$$(1-\lambda^2\nabla^2)\begin{pmatrix} B_{11}\dfrac{\partial^3 u_0}{\partial x^3}+(B_{12}+2B_{66})\dfrac{\partial^3 u_0}{\partial x \partial y^2} \\ +B_{22}\dfrac{\partial^3 v_0}{\partial y^3}+(B_{12}+2B_{66})\dfrac{\partial^3 v_0}{\partial x^2 \partial y} \\ -D_{11}\dfrac{\partial^4 w_b}{\partial x^4}-2(D_{12}+2D_{66})\dfrac{\partial^4 w_b}{\partial x^2 \partial y^2} \\ -D_{22}\dfrac{\partial^4 w_b}{\partial y^4}-D_{11}^s\dfrac{\partial^4 w_s}{\partial x^4} \\ -2(D_{12}^s+2D_{66}^s)\dfrac{\partial^4 w_s}{\partial x^2 \partial y^2}-D_{22}^s\dfrac{\partial^4 w_s}{\partial y^4} \end{pmatrix} + (1-\mu^2\nabla^2)\begin{pmatrix} -I_0(\ddot{w}_b+\ddot{w}_s)-I_1\left(\dfrac{\partial \ddot{u}_0}{\partial x}+\dfrac{\partial \ddot{v}_0}{\partial y}\right) \\ +I_2\nabla^2\ddot{w}_b+J_2\nabla^2\ddot{w}_s \\ -N^T\nabla^2(w_b+w_s) \end{pmatrix}=0 \tag{35}$$

$$(1-\lambda^2\nabla^2)\begin{pmatrix} B_{11}^s\dfrac{\partial^3 u_0}{\partial x^3}+(B_{12}^s+2B_{66}^s)\dfrac{\partial^3 u_0}{\partial x \partial y^2} \\ +B_{22}^s\dfrac{\partial^3 v_0}{\partial y^3}+(B_{12}^s+2B_{66}^s)\dfrac{\partial^3 v_0}{\partial x^2 \partial y} \\ -D_{11}^s\dfrac{\partial^4 w_b}{\partial x^4}-2(D_{12}^s+2D_{66}^s)\dfrac{\partial^4 w_b}{\partial x^2 \partial y^2} \\ -D_{22}^s\dfrac{\partial^4 w_b}{\partial y^4}-H_{11}^s\dfrac{\partial^4 w_s}{\partial x^4} \\ -2(H_{12}^s+2H_{66}^s)\dfrac{\partial^4 w_s}{\partial x^2 \partial y^2} \\ -H_{22}^s\dfrac{\partial^4 w_s}{\partial y^4}+A_{44}^s\nabla^2 w_s \end{pmatrix} + (1-\mu^2\nabla^2)\begin{pmatrix} -I_0(\ddot{w}_b+\ddot{w}_s)-J_1\left(\dfrac{\partial \ddot{u}_0}{\partial x}+\dfrac{\partial \ddot{v}_0}{\partial y}\right) \\ +J_2\nabla^2\ddot{w}_b+K_2\nabla^2\ddot{w}_s \\ -N^T\nabla^2(w_b+w_s) \end{pmatrix}=0 \tag{36}$$

3. Solution procedure

Exponential solution functions are assumed for displacement fields to solve the wave propagation of porous nanoplate with porosity analytically which are given in the following form

$$u_0 = Ue^{i(k_1x+k_2y-\omega t)} \tag{37a}$$

$$v_0 = Ve^{i(k_1x+k_2y-\omega t)} \tag{37b}$$

$$w_b = W_be^{i(k_1x+k_2y-\omega t)} \tag{37c}$$

$$w_s = W_se^{i(k_1x+k_2y-\omega t)} \tag{37d}$$

where U, V ; W_b and W_s denote the coefficients of wave amplitude, k_1, k_2 and ω indicate the wave numbers of wave dispersion along x and y directions and natural frequency, respectively.

By substituting Eqs. (35a)-(35d) into Eqs. (31)-(34) the eigenvalue equation can be obtained as

$$([K]_{4\times4} - \omega^2[M]_{4\times4})\begin{bmatrix} U \\ V \\ W_b \\ W_s \end{bmatrix} = 0 \tag{38}$$

in which K and M are stiffness and mass matrices, respectively. In order to obtain natural frequency of an eigenvalue problem, the following determinant must be set to zero, afterward wave frequency and phase velocity of FG porous nanoscale plate can be attained.

$$|[K - \omega^2M]_{4\times4}| = 0 \tag{39}$$

By setting $k_1 = k_2 = k$, the phase velocities of FG porous nanoplate can be expressed such as below

$$c_p = \frac{\omega}{k} \tag{40}$$

Moreover, the escape frequency of FG nanoplate can be derived by setting $\beta \to \infty$. Actually, it is obvious that the flexural waves won't propagate anymore after the escape frequency.

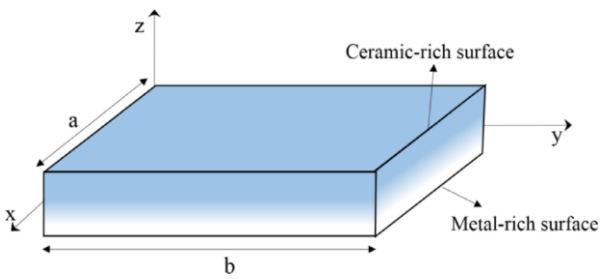

Fig. 1 Geometry of FG nanoplate

4. Numerical results and discussion

NSGT is extended for wave propagation analysis of FG porous nanoscale plate in a thermal environment. Moreover, the thickness of nanoplate which is illustrated in Fig. 1 is regarded as h = 100 nm. Also, a relative dimensionless size-dependent coefficient is presented for the sake of simplicity as

$$c = \frac{\lambda}{\mu} \tag{41}$$

where c is scale factor which will be utilized in the following illustrations. The validity of the proposed nonlocal strain gradient based plate model can be seen in the Fig. 2. In this diagram, the variation of the dimensionless natural frequency of a double nanoplate system against length scale parameter is drawn in order to show the accuracy of the presented methodology. As can be seen, answers achieved from our modeling are in an excellent agreement with those reported by Barati and Shahverdi (2017).

Fig. 3 indicates porosity coefficient effect on variation of phase velocity of porous nanoplate versus wave number for various gradient indices at ΔT = 100, c > 1. It is clear that by rising amount of wave number, the phase velocities of nanoplate increase. Furthermore, gradient index has decreasing effect such a way that in constant wave number and porosity coefficient, the highest phase velocity happens in the least gradient index and whenever gradient index is enlarged, the phase velocity is decreased. As can be seen, porosity has a notable effect on phase velocity. Also, in every gradient index, pure nanoplate possesses greater value than porous nanoplate. The reason for this behavior is that porosity makes nanostructure weaker.

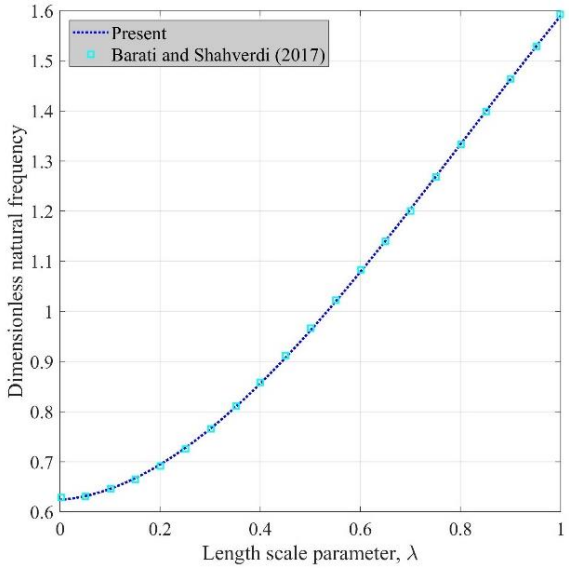

Fig. 2 Comparison of the natural frequency responses of FG double nanoplate systems with those presented in a formerly published paper by Barati and Shahverdi (2017) once a/h = 10, p = 1, and μ = 0.2

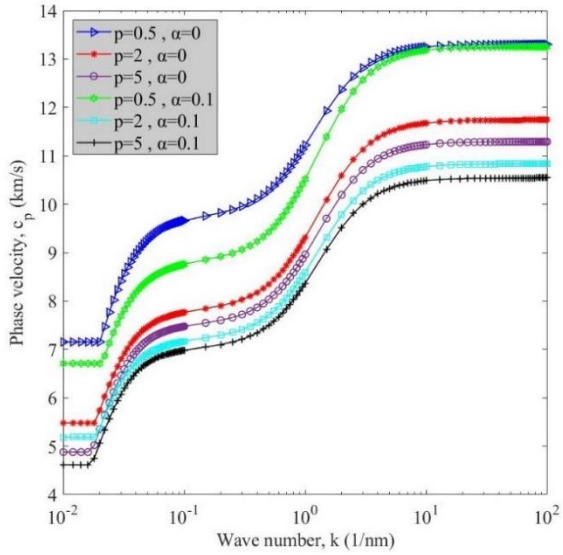

Fig. 3 Variation of phase velocity of porous nanoplate versus wave number for various gradient indices and porosity coefficients (ΔT = 100, c > 1)

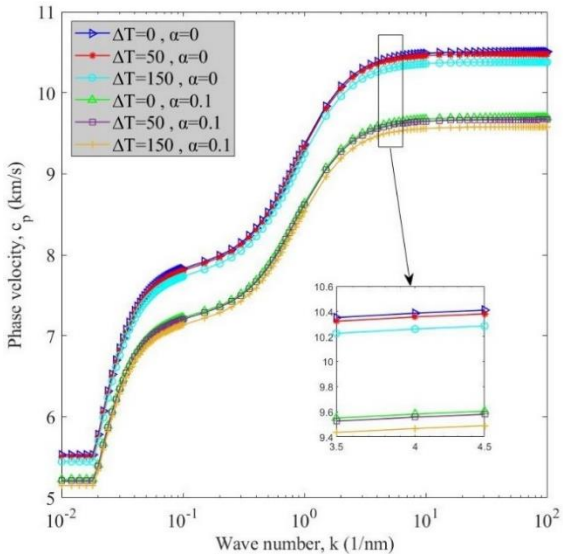

Fig. 4 The effect of porosity coefficient on variation of phase velocity versus wave number for various temperature differences (p = 2, c > 1)

The both effect of porosity coefficient and temperature change on variation of phase velocity versus wave number is shown in Fig. 4 at p = 2, c > 1. It can be inferred that the phase velocity has an inverse relation with temperature change and porosity coefficient. In constant porosity coefficient, by rising temperature change phase velocity of nanoplate is declined and this because of that stiffness of nanostructure decreases. Similar Fig. 2, by rising wave number and porosity coefficient, phase velocity value increases and decreases, respectively.

Variation of phase velocity versus wave number considering scale factors and porosity coefficients influences is demonstrated in Fig. 5 at ΔT = 100, p = 2. It can be observed obviously that in constant porosity coefficient, there are three different trends for phase velocity because of various scale factors. Once c > 1, the trend of diagram is ascending and phase velocity of nanoplate increases gradually. Once c = 1, at first, by rising wave number until k < 0.1 (1/nm) phase velocity increases and after k = 0.1 (1/nm) phase velocity remains at a constant value. The trend of c < 1 differs from others. In other word, after a gradual increase, the trend is descending and an increase in wave number resulted in a decrease in the amount of phase velocity. Plus, pure and porous diagrams have a same trend with a difference in amount of phase velocity which higher phase velocity happens in pure diagrams.

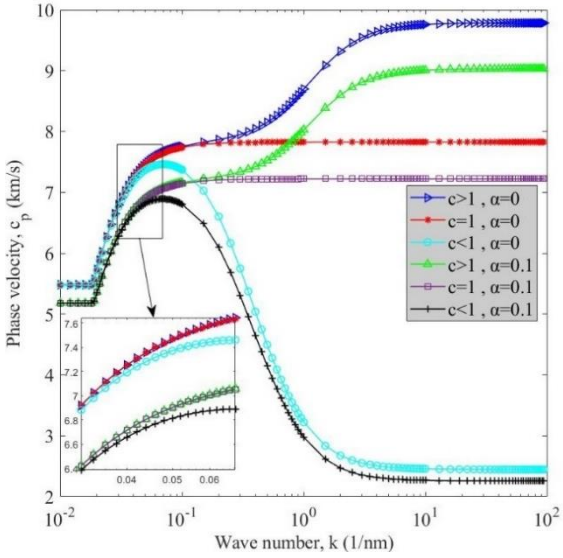

Fig. 5 Illustration of variation of phase velocity versus wave number for different scale factors and porosity coefficients (ΔT = 100, p = 2)

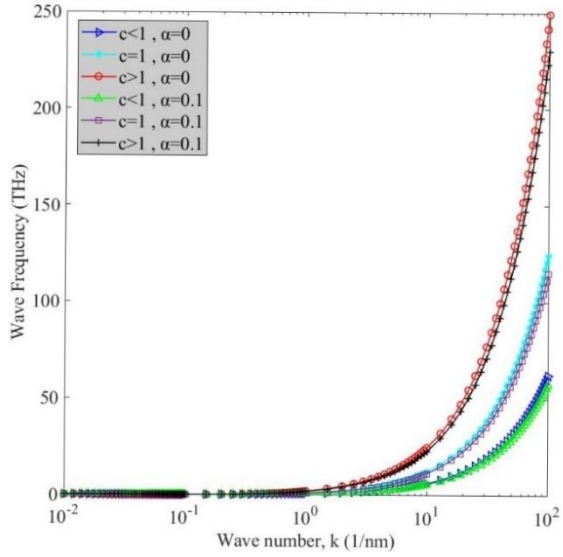

Fig. 6 Variation of wave frequency of porous nanoplate versus wave number for various scale factors and porosity coefficients (p = 2, ΔT = 100)

Fig. 6 reveals an illustration of variation of wave frequency versus wave number for different scale factors and porosity coefficients at $p = 2$, $\Delta T = 100$. According to this diagram, it can be inferred that whenever wave number raises, wave frequency enlarges with a slight slope and gradually, in higher wave numbers, wave frequency increases with a steep slope. In addition, wave frequency can be intensified while scale factor is assumed to be greater than one. As same as mentioned point about porosity effect in previous figures, in this diagram, the porosity has decreasing influence on amount of wave frequency.

The influence of temperature change on variation of wave frequency of nanoplate versus wave number for different porosity coefficients is depicted in Fig. 7 at $p = 2$, $c < 1$. The trend of this figure is similar to Fig. 6 and wave frequency has an uptrend. As can be seen, due to all diagrams are approximately same, the magnifier has been used in order to show more detail and clarify the effects of each parameter. Based on magnifying diagram, both temperature change and porosity coefficient possess decreasing effect. On the other hand, by rising temperature change while porosity coefficient is constant, wave frequency of nanoplate is lessened.

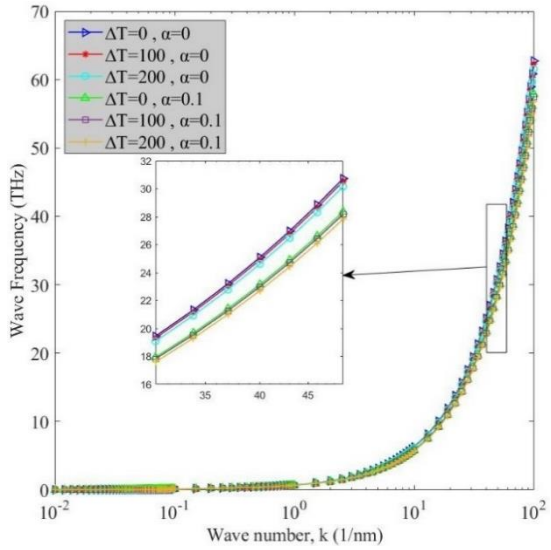

Fig. 7 Both effect of temperature differences and porosity coefficient on wave frequency of porous nanoplate versus wave number ($p = 2$, $c < 1$)

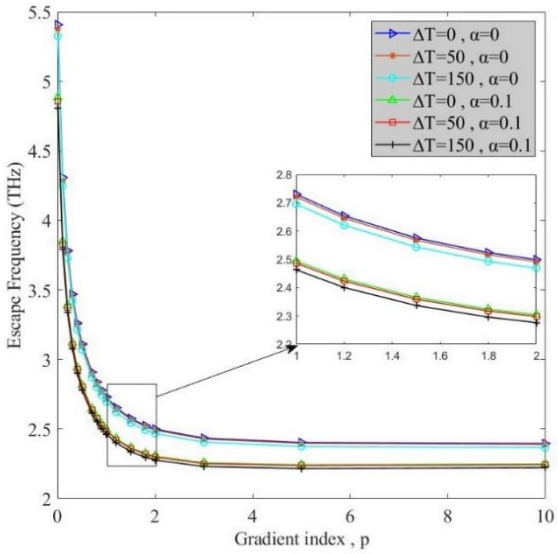

Fig. 8 Variation of escape frequency versus gradient index for different temperature differences and porosity coefficients ($c > 1$)

Variation of escape frequency versus gradient index for various temperature change and porosity coefficients is plotted in Fig. 8 at $c > 1$. In this diagram, magnifier can help us to realize better the effect of temperature change and porosity. It is obvious that both pure and porous material follow same trend. A decrease with a steep slope at first can be reported for pure and porous material and then every diagram leads to a constant value. The stiffness of nanoscale plate decreases owing to increase of the temperature change and porosity coefficient and because of that, the highest escape frequency is observed in pure material with low temperature change.

5. Conclusions

Wave dispersion of FG nanoscale plate in thermal environment considering porosity effect within the frameworks of a newly developed porosity-dependent homogenization technique by applying a refined plate theory is explored. NSGT is used to account for small scale effect and Hamilton's principle is employed in order to derive governing equation. Herein, the most important remarks are presented in review:

- The porosity has a remarkable effect on behavior of structure and also it must be regarded in design and analysis.
- The newly developed porosity homogenization method can cover better than conventional porosity-dependent homogenization methods by taking into account the coupling effects between Young's modulus and mass density.
- Thermal environment has decreasing influence on natural frequency of FG porous nanoplate.
- The wave frequency and phase velocity can be intensified by assuming a high value for scale factor.

References

Aydogdu, M. and Taskin, V. (2007), "Free vibration analysis of functionally graded beams with simply supported edges", *Mater. Des.*, **28**(5), 1651-1656. https://doi.org/10.1016/j.matdes.2006.02.007

Azadi, M. (2011), "Free and forced vibration analysis of fg beam considering temperature dependency of material properties", *J. Mech. Sci. Technol.*, **25**(1), 69-80. https://doi.org/10.1007/s12206-010-1015-y

Barati, M.R. (2017), "On wave propagation in nanoporous materials", *Int. J. Eng. Sci.*, **116**, 1-11. https://doi.org/10.1016/j.ijengsci.2017.03.007

Barati, M.R. (2018), "A general nonlocal stress-strain gradient

theory for forced vibration analysis of heterogeneous porous nanoplates", *Eur. J. Mech. - A/Solids*, **67**, 215-230. https://doi.org/10.1016/j.euromechsol.2017.09.001

Barati, M.R. and Shahverdi, H. (2017), "Hygro-thermal vibration analysis of graded double-refined-nanoplate systems using hybrid nonlocal stress-strain gradient theory", *Compos. Struct.*, **176**, 982-995. https://doi.org/10.1016/j.compstruct.2017.06.004

Chen, H., Wang, A., Hao, Y. and Zhang, W. (2017), "Free vibration of fgm sandwich doubly-curved shallow shell based on a new shear deformation theory with stretching effects", *Compos. Struct.*, **179**, 50-60. https://doi.org/10.1016/j.compstruct.2017.07.032

Daneshmehr, A., Rajabpoor, A. and Hadi, A. (2015), "Size dependent free vibration analysis of nanoplates made of functionally graded materials based on nonlocal elasticity theory with high order theories", *Int. J. Eng. Sci.*, **95**, 23-35. https://doi.org/10.1016/j.ijengsci.2015.05.011

Ebrahimi, F. and Barati, M.R. (2017), "A nonlocal strain gradient refined beam model for buckling analysis of size-dependent shear-deformable curved fg nanobeams", *Compos. Struct.*, **159**, 174-182. https://doi.org/10.1016/j.compstruct.2016.09.058

Ebrahimi, F. and Dabbagh, A. (2017), "On flexural wave propagation responses of smart fg magneto-electro-elastic nanoplates via nonlocal strain gradient theory", *Compos. Struct.*, **162**, 281-293. https://doi.org/10.1016/j.compstruct.2016.11.058

Ebrahimi, F. and Haghi, P. (2017), "Wave propagation analysis of rotating thermoelastically-actuated nanobeams based on nonlocal strain gradient theory", *Acta Mechanica Solida Sinica*, **30**(6), 647-657. https://doi.org/10.1016/j.camss.2017.09.007

Ebrahimi, F., Barati, M.R. and Dabbagh, A. (2016a), "A nonlocal strain gradient theory for wave propagation analysis in temperature-dependent inhomogeneous nanoplates", *Int. J. Eng. Sci.*, **107**, 169-182. https://doi.org/10.1016/j.ijengsci.2016.07.008

Ebrahimi, F., Ghasemi, F. and Salari, E. (2016b), "Investigating thermal effects on vibration behavior of temperature-dependent compositionally graded euler beams with porosities", *Meccanica*, **51**(1), 223-249. https://doi.org/10.1007/s11012-015-0208-y

Ebrahimi, F., Barati, M.R. and Haghi, P. (2017a), "Thermal effects on wave propagation characteristics of rotating strain gradient temperature-dependent functionally graded nanoscale beams", *J. Thermal Stress.*, **40**(5), 535-547. https://doi.org/10.1080/01495739.2016.1230483

Ebrahimi, F., Jafari, A. and Barati, M.R. (2017b), "Vibration analysis of magneto-electro-elastic heterogeneous porous material plates resting on elastic foundations", *Thin-Wall. Struct.*, **119**, 33-46. https://doi.org/10.1016/j.tws.2017.04.002

Ebrahimi, F., Barati, M.R. and Dabbagh, A. (2018a), "Wave propagation in embedded inhomogeneous nanoscale plates incorporating thermal effects", *Waves Random Complex Media*, **28**(2), 215-235. https://doi.org/10.1080/01495739.2016.1230483

Ebrahimi, F., Barati, M.R. and Haghi, P. (2018b), "Wave propagation analysis of size-dependent rotating inhomogeneous nanobeams based on nonlocal elasticity theory", *J. Vib. Control*, **24**(17), 3809-3818. https://doi.org/10.1177/1077546317711537

Ebrahimi, F., Dehghan, M. and Seyfi, A. (2019a), "Eringen's nonlocal elasticity theory for wave propagation analysis of magneto-electro-elastic nanotubes", *Adv. Nano Res., Int. J.*, **7**(1), 1-11. https://doi.org/10.12989/anr.2019.7.1.001

Ebrahimi, F., Seyfi, A. and Dabbagh, A. (2019b), "A novel porosity-dependent homogenization procedure for wave dispersion in nonlocal strain gradient inhomogeneous nanobeams", *Eur. Phys. J. Plus*, **134**(5), 226. https://doi.org/10.1140/epjp/i2019-12547-8

Eltaher, M.A., Fouda, N., El-midany, T. and Sadoun, A.M. (2018), "Modified porosity model in analysis of functionally graded porous nanobeams", *J. Brazil. Soc. Mech. Sci. Eng.*, **40**(3), 141. https://doi.org/10.1007/s40430-018-1065-0

Fan, Y., Xiang, Y. and Shen, H.-S. (2018), "Nonlinear forced vibration of fg-grc laminated plates resting on visco-pasternak foundations", *Compos. Struct.*, **209**, 443-452. https://doi.org/10.1016/j.compstruct.2018.10.084

Fuschi, P., Pisano, A.A. and Polizzotto, C. (2019), "Size effects of small-scale beams in bending addressed with a strain-difference based nonlocal elasticity theory", *Int. J. Mech. Sci.*, **151**, 661-671. https://doi.org/10.1016/j.ijmecsci.2018.12.024

Ghayesh, M.H. and Farajpour, A. (2018), "Nonlinear mechanics of nanoscale tubes via nonlocal strain gradient theory", *Int. J. Eng. Sci.*, **129**, 84-95. https://doi.org/10.1016/j.ijengsci.2018.04.003

Hebali, H., Tounsi, A., Houari, M.S.A., Bessaim, A. and Bedia, E.A.A. (2014), "New quasi-3d hyperbolic shear deformation theory for the static and free vibration analysis of functionally graded plates", *J. Eng. Mech.*, **140**(2), 374-383. https://doi.org/10.1061/(ASCE)EM.1943-7889.0000665

Hosseini, S. and Rahmani, O. (2016), "Free vibration of shallow and deep curved fg nanobeam via nonlocal timoshenko curved beam model", *Appl. Phys. A*, **122**(3), 169. https://doi.org/10.1007/s00339-016-9696-4

Keleshteri, M., Asadi, H. and Wang, Q. (2017), "Large amplitude vibration of fg-cnt reinforced composite annular plates with integrated piezoelectric layers on elastic foundation", *Thin-Wall. Struct.*, **120**, 203-214. https://doi.org/10.1016/j.tws.2017.08.035

Li, L., Hu, Y. and Ling, L. (2015), "Flexural wave propagation in small-scaled functionally graded beams via a nonlocal strain gradient theory", *Compos. Struct.*, **133**, 1079-1092. https://doi.org/10.1016/j.compstruct.2015.08.014

Lu, L., Guo, X. and Zhao, J. (2019), "A unified size-dependent plate model based on nonlocal strain gradient theory including surface effects", *Appl. Math. Model.*, **68**, 583-602. https://doi.org/10.1016/j.apm.2018.11.023

Lv, Z., Qiu, Z., Zhu, J., Zhu, B. and Yang, W. (2018), "Nonlinear free vibration analysis of defective fg nanobeams embedded in elastic medium", *Compos. Struct.*, **202**, 675-685. https://doi.org/10.1016/j.compstruct.2018.03.068

Mahinzare, M., Jannat Alipour, M., Sadatsakkak, S.A. and Ghadiri, M. (2019), "A nonlocal strain gradient theory for dynamic modeling of a rotary thermo piezo electrically actuated nano fg circular plate", *Mech. Syst. Signal Process.*, **115**, 323-337. https://doi.org/10.1016/j.ymssp.2018.05.043

Mirjavadi, S.S., Afshari, B.M., Barati, M.R. and Hamouda, A.M. S. (2019), "Transient response of porous fg nanoplates subjected to various pulse loads based on nonlocal stress-strain gradient theory", *Eur. J. Mech. - A/Solids*, **74**, 210-220. https://doi.org/10.1016/j.euromechsol.2018.11.004

Mohammadi, M., Mohseni, E. and Moeinfar, M. (2019), "Bending, buckling and free vibration analysis of incompressible functionally graded plates using higher order shear and normal deformable plate theory", *Appl. Math. Model.*, **69**, 47-62. https://doi.org/10.1016/j.apm.2018.11.047

Phung-Van, P., Thai, C.H., Nguyen-Xuan, H. and Abdel Wahab, M. (2019), "Porosity-dependent nonlinear transient responses of functionally graded nanoplates using isogeometric analysis", *Compos. Part B: Eng.*, **164**, 215-225. https://doi.org/10.1016/j.compositesb.2018.11.036

Pourjabari, A., Hajilak, Z.E., Mohammadi, A., Habibi, M. and Safarpour, H. (2019), "Effect of porosity on free and forced vibration characteristics of the gpl reinforcement composite nanostructures", *Comput. Math. Appl.*, **77**(10), 2608-2626. https://doi.org/10.1016/j.camwa.2018.12.041

Sahmani, S. and Aghdam, M.M. (2018), "Nonlocal strain gradient shell model for axial buckling and postbuckling analysis of

magneto-electro-elastic composite nanoshells", *Compos. Part B: Eng.*, **132**, 258-274. https://doi.org/10.1016/j.compositesb.2017.09.004

Shahsavari, D., Shahsavari, M., Li, L. and Karami, B. (2018), "A novel quasi-3d hyperbolic theory for free vibration of fg plates with porosities resting on winkler/pasternak/kerr foundation", *Aerosp. Sci. Technol.*, **72**, 134-149. https://doi.org/10.1016/j.ast.2017.11.004

Shojaeian, M., Beni, Y.T. and Ataei, H. (2016), "Electro-mechanical buckling of functionally graded electrostatic nanobridges using strain gradient theory", *Acta Astronautica*, **118**, 62-71. https://doi.org/10.1016/j.actaastro.2015.09.015

Şimşek, M. (2016), "Nonlinear free vibration of a functionally graded nanobeam using nonlocal strain gradient theory and a novel hamiltonian approach", *Int. J. Eng. Sci.*, **105**, 12-27. https://doi.org/10.1016/j.ijengsci.2016.04.013

Şimşek, M. and Reddy, J. (2013), "Bending and vibration of functionally graded microbeams using a new higher order beam theory and the modified couple stress theory", *Int. J. Eng. Sci.*, **64**, 37-53. https://doi.org/10.1016/j.ijengsci.2012.12.002

Tan, Z.-Q. and Chen, Y.-C. (2019), "Size-dependent electro-thermo-mechanical analysis of multilayer cantilever microactuators by joule heating using the modified couple stress theory", *Compos. Part B: Eng.*, **161**, 183-189. https://doi.org/10.1016/j.compositesb.2018.10.067

Thanh, N.V., Khoa, N.D., Tuan, N.D., Tran, P. and Duc, N.D. (2017), "Nonlinear dynamic response and vibration of functionally graded carbon nanotube-reinforced composite (fg-cntrc) shear deformable plates with temperature-dependent material properties and surrounded on elastic foundations", *J. Thermal Stress.*, **40**(10), 1254-1274. https://doi.org/10.1080/01495739.2017.1338928

Zeighampour, H., Tadi Beni, Y. and Botshekanan Dehkordi, M. (2018), "Wave propagation in viscoelastic thin cylindrical nanoshell resting on a visco-pasternak foundation based on nonlocal strain gradient theory", *Thin-Wall. Struct.*, **122**, 378-386. https://doi.org/10.1016/j.tws.2017.10.037

Zeng, S., Wang, B.L. and Wang, K.F. (2019), "Nonlinear vibration of piezoelectric sandwich nanoplates with functionally graded porous core with consideration of flexoelectric effect", *Compos. Struct.*, **207**, 340-351. https://doi.org/10.1016/j.compstruct.2018.09.040

Zok, F.W. and Levi, C.G. (2001), "Mechanical properties of porous-matrix ceramic composites", *Adv. Eng. Mater.*, **3**(1-2), 15-23. https://doi.org/10.1002/1527-2648(200101)3:1/2<15::AID-ADEM15>3.0.CO;2-A

CC